American Mineralogist, Volume 59, pages 700–708, 1974

Synthesis and Study of Gadolinites

JUN ITO

Department of Geological Sciences, Harvard University, Cambridge, Massachusetts 02138

AND STEFAN S. HAFNER

Department of Geosciences, University of Marburg, D-3550 Marburg-Lahn, West Germany

Abstract

Solid-solutions in a three component system of the type gadolinite ($Fe^{2+}Ln^{3+}{}_2Be_2Si_2O_{10}$)-calciogadolinite ($Fe^{3+}CaLn^{3+}Be_2Si_2O_{10}$)-($H_2Ln^{3+}{}_2Be_2Si_2O_{10}$) are called gadolinites. The solid-solution series probably are partial.

Mössbauer spectra of $Fe^{2+}Y_2Be_2Si_2O_{10}$, synthesized at 720°C under total P_{H_2O} = 2 kbar and of $Fe^{3+}CaYBe_2Si_2O_{10}$ obtained by heating the gel at 1150°C in air, confirm the existence of distorted octahedra about Fe^{2+} and Fe^{3+} that were inferred from interatomic distances obtained by X-ray diffraction methods. The infrared spectrum of $H_2Y_2Be_2Si_2O_{10}$, crystallized at 600°C under total P_{H_2O} = 2 kbar, shows strong OH absorption peaks at 3550 and 650 cm^{-1}. Using $Na_2W_2O_7$ as a flux, we have grown small single crystals of various chemical compositions by slow cooling of the solution from 1250°C to 700°C. Green crystals of $CuPr_2Be_2Si_2O_{10}$, isostructural with gadolinite, grew up to 3 mm in length.

Introduction

Previous studies of gadolinites revealed two distinct subspecies. These are calciogadolinite—$M^{3+}CaLn^{3+}Be_2Si_2O_{10}$ where M = Fe and Ga, and Ln = lanthanides and Y (Nakai, 1938; Ito, 1967)—and $H_2Ln^{3+}{}_2Be_2Si_2O_{10}$, an unnamed mineral described by Semenov, Dusmatov and Samsonova, (1963) and by Ito (1965). The latter is isostructural with datolite, $H_2Ca_2B_2Si_2O_{10}$ (Ito and Mori, 1953; Pavlov and Belov, 1959; Pant and Cruickshank, 1967). An intermediate member between $H_2Ln^{3+}{}_2Be_2Si_2O_{10}$ and datolite has been found from Tadzhik, USSR (Semenov, Dusmatov, and Samsonova, 1963).

Homilite, which has the idealized formula $Fe^{2+}Ca_2B_2Si_2O_{10}$ (Paikjull, 1876), is supposedly an anhydrous datolite filled with Fe^{2+} or boron analog of gadolinite $Fe^{2+}Ln^{3+}{}_2Be_2Si_2O_{10}$. The natural homilites, however, including that from the original locality, have been shown to contain a significant amount of Be and lanthanides. Therefore the existence of the pure homilite end member is in doubt. Erdmanite, $Fe^{2+}CaLn^{3+}Be_2Si_2O_{10}$ (Engström, 1877; Des Cloizeaux and Damour, 1877; Brögger, 1890), has an intermediate composition between gadolinite and homilite. Homilite in contrast to erdmanite has been known to contain more Y-group lanthanides than Ce-group lanthanides. New analyses of gadolinites from USSR (Aleksandrova *et al,* 1966) gave appreciable amounts of B_2O_3 up to 4.98 wt percent in the minerals. These amounts indicate that partial solid-solution between gadolinite and erdmanite exists.

To clarify compositional relationship of the minerals given in Table 1 was one aim of the present study. Naturally occurring gadolinites almost always contain CaO, Fe_2O_3 and H_2O. The mean values for 44 available analyses (Dana, 1900; Nagashima and Nagashima, 1960; Aleksandrova *et al,* 1966) gave CaO = 0.97, Fe_2O_3 = 2.68 and $H_2O(+)$ = 0.92 wt percent. Gadolinites containing the highest reported amounts of $H_2O(+)$ come from Sweden at Storna Tuna Parlisch (2.38 wt percent; see Lindstrom, 1874) and at Mälo (3.36 wt percent; see Petersson, 1890. We suggest defining naturally occurring boron-free gadolinites as any solid-solution of the three end-members as shown in Figure 1. In this ternary system there may be a large phase gap present.

It was also decided to examine the Mössbauer spectra of both ferrous yttrium gadolinite and ferric yttrium calcio gadolinite in order to substantiate ferrous-ferric iron replacement in the octahedrally coordinated sites, and to ascertain whether the octa-

TABLE 1. Compositional Relationships of the Minerals Belonging to the Gadolinite-Datolite Group

DATOLITE	HOMILITE	
$H_2Ca_2B_2Si_2O_{10}$	$Fe^{2+}Ca_2B_2Si_2O_{10}$	
Unnamed Mineral Tadzhik, USSR	ERDMANITE	
$H_2CaLn^{3+}BeBSi_2O_{10}$	$Fe^{2+}Ln^{3+}CaBeBSi_2O_{10}$	
Unnamed Mineral Tuva, USSR	GADOLINITE	CALCIOGADOLINITE
$H_2Ln_2^{3+}Be_2Si_2O_{10}$	$Fe^{2+}Ln_2^{3+}Be_2Si_2O_{10}$	$Fe^{3+}CaLn^{3+}Be_2Si_2O_{10}$

hedral distortion indicated by Mössbauer spectra are consistent with the existing structural data. Infrared spectra of the gadolinites and related minerals are quite similar (Fig. 2).

Some details of flux growth of the single crystals, hydrothermal synthesis, and gel preparation will also be described.

Method of Synthesis and Growth

Synthesis of the Pure Yttrium Gadolinite Solid-Solution Series

Basic starting materials of amorphous hydrated beryllosilicates were prepared. The gels were precipitated by adding ammonia (to achieve a pH of 10) to solutions containing stoichiometric amounts of beryllium nitrate, yttrium chloride, (ferric chloride in the case of calciogadolinite), and a silicic acid

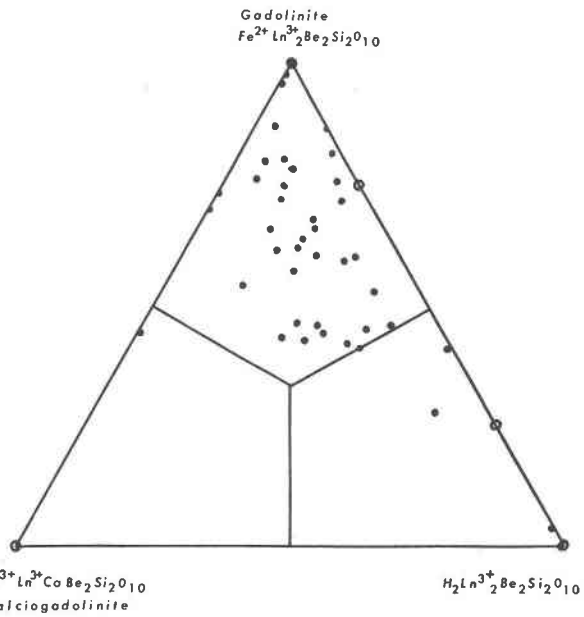

FIG. 1. Compositional plots of the chemical analyses of the 44 gadolinites on the triangular diagram for the system $Fe^{2+}Ln^{3+}{}_2Be_2Si_2O_{10}$–$Fe^{3+}LnCaBe_2Si_2O_{10}$–$H_2Ln_2Be_2Si_2O_{10}$ (Ln = lanthanides and Y). The plots were made in terms of molecular ratio of FeO, $FeO_{1.5}$, and H_2O in the chemical analyses.

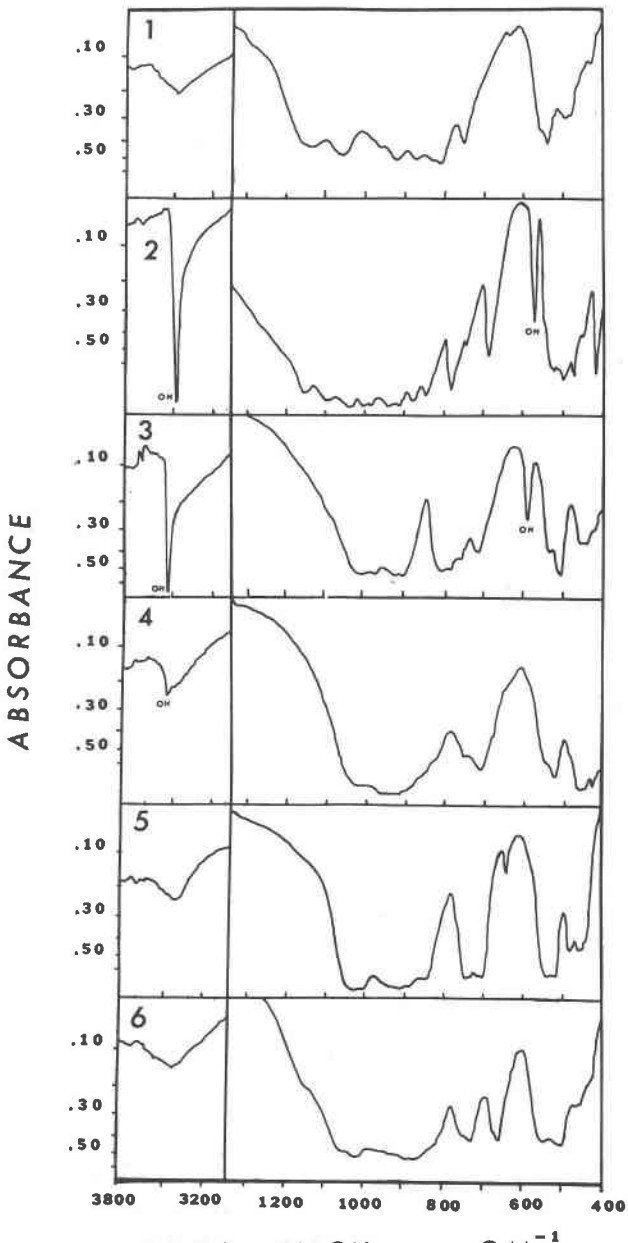

FIG. 2. Infrared spectra of natural gadolinite, synthetic analogs, and its related compounds: 1. Homilite, $Fe^{2+}(LnCa)_2(B,Be)_2Si_2O_{10}$ from Langesundfjord, Norway, H.M. 89603. 2. Datolite, $H_2Ca_2B_2Si_2O_{10}$ from Westfield, Massachusetts, H.M. 95455. 3. $H_2Y_2Be_2Si_2O_{10}$, synthesized at 600°C and P_{H_2O} = 2kbar. 4. Gadolinite from Iveland, Norway, H.M. 107360. 5. $Fe^{2+}Y_2Be_2Si_2O_{10}$ synthesized at 720°C and P_{H_2O} = 2 kbar. 6. $Fe^{3+}CaYBe_2Si_2O_{10}$, calciogadolinite synthesized at 1250°C in air from gel.

TABLE 2. Unit-Cell Dimensions of Synthetic Yttrium Gadolinite, Calciogadolinite, and Hydrogadolinite Obtained from Least-Squares Refinement of X-Ray Diffraction Data, Cu$K\alpha$

Formula	a	b	c	β	Vol.	Synthesis conditions
$MnY_2Be_2Si_2O_{10}$	10.006(1)	7.4809(7)	4.7558(5)	89°38'(1')	356.0(1)	1250°C, in air, 48h
$Fe^{2+}Y_2Be_2Si_2O_{10}$	9.920(4)	7.4843(2)	4.7474(7)	89°36'(2')	351.7(2)	740°C, 2kb P_{H_2O}, 48h
						1050°C in H_2 10% N_2 90% 1 atm.
$ZnY_2Be_2Si_2O_{10}$	9.932(2)	7.490(1)	4.7284(7)	89°36'(1')	351.8(1)	1250°C, in air, 48h
$CoY_2Be_2Si_2O_{10}$	9.936(1)	7.4747(7)	4.7209(4)	89°56'(1')	350.6(4)	1250°C, in air, 48h
$CuY_2Be_2Si_2O_{10}$	9.885(1)	7.5043(8)	4.7289(9)	89°24'(1')	350.8(1)	Flux grown 1250°C-750°C
$MgY_2Be_2Si_2O_{10}$	9.941(3)	7.463(1)	4.703(1)	90°1'(1')	348.9(1)	1250°C, in air, 48h
$NiY_2Be_2Si_2O_{10}$	9.911(4)	7.447(2)	4.694(2)	90°0'(2')	346.5(2)	1250°C, in air, 48h
$Fe^{3+}YCaBe_2Si_2O_{10}$	9.988(2)	7.566(2)	4.696(1)	90°1'(2')	354.0(2)	1150°C, in air, 48h
$H_2Y_2Be_2Si_2O_{10}$	9.861(4)	7.605(2)	4.720(2)	89°39'(2')	354.0(2)	600°C, 2kb P_{H_2O}, 72h
$Fe^{2+}_{.75}H_{0.5}Y_2Be_2Si_2O_{10}$*	9.916(7)	7.544(5)	4.740(3)	89°42'(3')	354.6(2)	600°C, 2kb P_{H_2O}, 72h
$Fe^{2+}_{.25}H_{1.5}Y_2Be_2Si_2O_{10}$*	9.879(4)	7.592(3)	4.727(2)	89°2'(2')	354.5(2)	600°C, 2kb P_{H_2O}, 72h

*Starting compositions only.
The estimated standard deviations are given in parentheses and refer to last digit quoted.

solution. The resulting precipitates were centrifuged, washed with 1 percent ammonia solution, and centrifuged once more. Finally, the gels were air dried.

A stoichiometric amount of ferrous oxalate or $Ca(OH)_2$ was then placed in an agate mortar with the dried gels and thoroughly mixed. Upon heating, simple mixtures of oxides and hydroxides of the gadolinite compositions often crystallized as silicate oxyapatites or as other phases. Preparation of the amorphous beryllosilicates seems necessary for the crystallization of certain gadolinites.

The hydrothermal syntheses were carried out in cold-seal hydrothermal bombs made of stellite. The silver container was made by multiple folding of silver foil (50 mm × 50 mm × 0.03 mm). A small amount of *l*-ascorbic acid was added to the container in order to maintain low oxygen fugacities. A partial solid-solution series between $Fe^{2+}Y_2Be_2Si_2O_{10}$ and $H_2Y_2Be_2Si_2O_{10}$ with a possible unmixing gap in the middle have been obtained at 600°C, $P_{H_2O} = 2$ kbar and 72 hours (Table 2).

Hydrothermally crystallized $Fe^{2+}Y_2Be_2Si_2O_{10}$ (700°C, 2 kbar and 48 hours) gave weak infrared OH absorption at 3550 cm^{-1}. The absorption peak disappeared after the sample was heated at 1050°C in an atmosphere of 10 percent vol. H_2 and 90 percent N_2 for three hours.

The $H_2Y_2Be_2Si_2O_{10}$ obtained at 600°C, 2 kbar and 72 hours, corresponds to the mineral from Tuva, USSR, described by Semenov, Dusmatov, and Samsonova (1963). After heating in air at 1000°C, it lost H_2O (6.71 wt percent) and formed β-$Y_2Si_2O_7$ and BeO.

Calciogadolinite has been synthesized in air at 1180°C for 72 hours. The charge was ground once after the initial 24 hour period of heating. No attempt was made to synthesize intermediate compounds for the solid solution between gadolinite and calciogadolinite because of the difficulty in maintaining correct Fe^{2+}/Fe^{3+} ratio in the runs. However, the presence of the above solid solution series seems probable. Non-ferrous polycrystalline gadolinite analogs were crystallized by heating the gels at 1250°C in air for 48 hours.

Single Crystal Growth Using Flux

Sodium ditungstate, $Na_2W_2O_7$, has been used as a high temperature solvent. The molecular ratio for the charges and the solvent was approximately as follows. $M^{2+}Ln^{3+}{}_2Be_2Si_2O_{10}:SiO_2:Na_2W_2O_7 = 2:1:5$. The following reagents were used to make up the charges: BeO, H_2SiO_3, Y_2O_3 and other lanthanide oxides, $NiCO_3$, $CoCO_3$, ZnO, and $CuCO_3$.

The charges were mixed and placed in platinum crucibles of 50 cm^3 capacity, and then heated up to 1280°C in a furnace with silicon-carbide heating

rods. The resulting melts were equilibrated for a period of four days, and then cooled down slowly to 750°C at the rate of 2°C per hour. The heating of the charges ended at 750°C and the furnace was brought to room temperature by natural cooling. The remaining sodium tungstate was dissolved in a 5 percent solution of hot dilute NaOH, and washed away. Crystalline products recovered from the residue include euhedral gadolinites, phenacite, Ni,Co, or Zn tungstates, $NaLn(WO_4)_2$, and some unidentified phases. The end products were always mixtures, but the gadolinite crystals were easily distinguished and hand picked under binocular.

The following crystals have been grown so far. Colors, maximum length in mm, and β angles measured on *b*-axis precession photographs are given in parentheses. $CuPr_2Be_2Si_2O_{10}$ (emerald green, 3 mm 90°39′), $CuNd_2Be_2Si_2O_{10}$ (green, 3 mm, 90°20′), $CuSm_2Be_2Si_2O_{10}$ (light green, 1.5 mm, 90°10′), $CuSmGdBe_2Si_2O_{10}$ (light blue, 1.5 mm, 89°50′), $CuGd_2Be_2Si_2O_{10}$ (light blue, 1 mm, 89°30′), $CuDy_2Be_2Si_2O_{10}$ (light blue, 0.5 mm, 89°15′), $CuY_2Be_2Si_2O_{10}$ (light blue, 1 mm, 89°20′), $CuYb_2Be_2Si_2O_{10}$ (light blue, 0.3 mm, 88°55′), $ZnDy_2Be_2Si_2O_{10}$ (pale yellow, 0.2 mm, 90°5′), $CoDy_2Be_2Si_2O_{10}$ (amber yellow, 0.1 mm, 90°5′), $NiY_2Be_2Si_2O_{10}$ (light blue, 0.2 mm, 90°6′) and $NiYb_2Be_2Si_2O_{10}$ (yellowish green, 1 mm, 89°45′).

Infrared Spectra

Infrared spectra using the KBr disk method were taken (Fig. 2) for (1) a gadolinite from Iveland, Norway (H.M. 107360), treated hydrothermally at 700°C, P_{H_2O} = 2 kbar for 24 hours under reducing conditions, (2) a synthetic ferrous yttrium gadolinite, (3) a synthetic ferric yttrium calciogadolinite, and (4) a synthetic $H_2Y_2Be_2Si_2O_{10}$. The spectra of datolite, $H_2Ca_2B_2Si_2O_{10}$, from Westfield, Massachusetts (H.M. 95455), and homilite, $Fe^{2+}(Ca,Ln^{3+})_2(Be,B)_2Si_2O_{10}$, from Langesundfjord, Sweden (H.M. 89603), are also shown in Figure 2. The spectra prove that homilite and datolite are closely related, and homilite has in fact the Fe^{2+}-filled datolite structure. It is noted that this particular specimen from Langesundfjord contained a significant amount of beryllium oxide and yttria earths.

Very strong and sharp OH absorption peaks at 3550 and 560 cm^{-1} have been observed in datolite containing 5.6 wt percent H_2O (computed) and in synthetic $H_2Y_2Be_2Si_2O_{10}$ containing 6.71 wt percent H_2O (meas).

Major infrared absorption spectra in the range of 400–1300 cm^{-1} are rather similar in all the above compounds. The doublets observed in all the specimens at the range 455–465 cm^{-1} have been identified as the absorption of the SiO_4 tetrahedra, and the strong absorption at 940–950 cm^{-1} has also been assigned to the Si-O bonds (Alexandrova *et al*, 1966). No further attempts have been made at this stage to assign all these absorptions to certain structural bonds of the gadolinite type structure, because of the rather complex chemical compositions and structures of these minerals.

X-Ray Studies

Most natural gadolinites occur in a metamict state. During hydrothermal crystallization under strongly reducing conditions, these near-amorphous black metamict crystals become colorless transparent crystals which give very sharp X-ray diffraction patterns. This change may be brought about for example, at 700°C, P_{H_2O} = 2kbar and 24 hours with a small amount of *l*-ascorbic acid. Natural gadolinites always contain the entire series of lanthanides, different divalent ions, and often Zr^{4+} and Th^{4+}. For the purpose of the X-ray structure refinements or studies of the physical properties, however, the synthesis of single crystals is highly desirable.

All synthetic gadolinite crystals in this work have been studied with the X-ray precession method using Mo$K\alpha$ radiation. In all cases, the space group has been found to be $P2_1/c$, which is the same as that assigned to the natural mineral. The β angles for the gadolinites vary systematically from 89° to 92° depending on the concentrations of divalent cations and lanthanide ions (Ito, 1965). This dependence of the β angles has been closely investigated in the Cu-lanthanides gadolinite series. In this series β angles will reach approximately 90°0′ at the composition $CuSm_{1.33}Gd_{0.66}Be_2Si_2O_{10}$, but X-ray diffraction intensities on the reciprocal plane normal to the *b* axis do not acquire additional symmetry. This observation was also confirmed with the intensities of the 402, $\bar{4}0\bar{2}$, $\bar{4}02$, $40\bar{2}$ reflections on precession photographs of ZnDy and CoDy gadolinites. In both crystals, the β angles measure 90°0′ ± 5′. We believe, therefore, that mirror plane symmetry parallel to *b* will not be found in any existing solid solution regardless of its chemical composition, and the pseudosymmetry of intensities is the more pronounced the more β departs from 90°.

The octahedron in gadolinite is strongly distorted

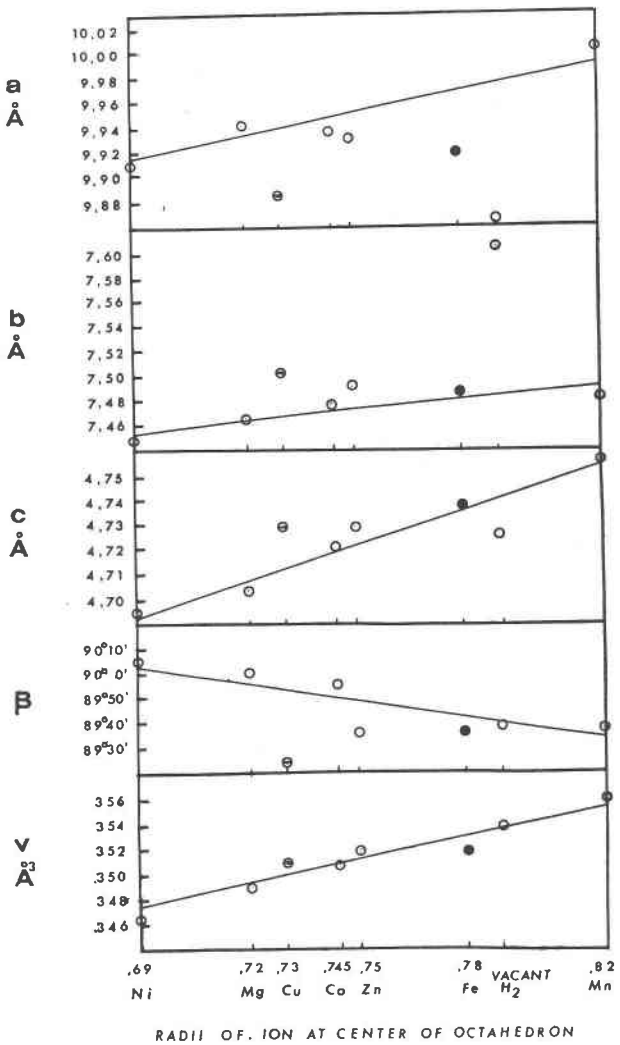

FIG. 3. Unit-cell dimensions of the synthetic yttrium analogs of gadolinites *vs* ionic radii of the divalent cation (Shannon and Prewitt, 1969).

(Ito and Mori, 1953). It seems extremely accommodating because a large variety of cations from Cd^{2+} (0.95 Å) to Ni^{2+} (0.69 Å) enter this site (Ito, 1965). Refined unit-cell dimensions (Table 2) of all the yttrium analogs have been plotted in Figure 3 in terms of ionic radii as given by Shannon and Prewitt (1969). The unit-cell volume for the $H_2Y_2Be_2Si_2O_{10}$ having vacant octahedral sites and stabilized with two OH^- falls between those of Fe^{2+} and Mn^{2+} analogs. The octahedron evidently stretches when occupied by larger (over 0.80 Å) cations, and shrinks when accommodating smaller divalent cations (smaller than 0.80 Å).

It has been demonstrated that simple plots of unit-cell dimensions of the analogous compounds against corresponding ionic radii reveal distortion of oxygen tetrahedra of certain metals in crystals (Ito and Peiser, 1969). In a previous study (Ito, 1965) of the synthetic analogs of gadolinites, Cu^{2+} and Fe^{2+} showed rather peculiar variations of the unit-cell dimensions, particularly in their β angles versus ionic radii of Ahrens (1952). Refined unit-cell dimensions of the pure synthetic yttrium analogs with different cations were plotted against the more recently published ionic radii by Shannon and Prewitt (1969). The plots seem to demonstrate, as expected, the effects of the distorted octahedra occupied by Cu^{2+} and Fe^{2+} (Jahn and Teller, 1937) in the gadolinite structure. Furthermore, the above plots clearly show distortion of the unit-cell when these octahedral sites are occupied by cations preferring distorted sites such as Cu^{2+} and Fe^{2+}. Moreover, the departure of each unit-cell dimension is consistent with individual characteristics of these cations. Cu^{2+} analogs with deformed octahedra show distortions in three directions to point symmetry *mmm*, while Fe^{2+} analogs with compressed octahedra demonstrated only departures in one direction to point symmetry $4/mmm$. The unit cell dimensions of the other divalent cation analogs (Mn^{2+}, Co^{2+}, Mg^{2+}, and Ni^{2+}) can be correlated with the ionic radii on an almost linear basis. However, the Zn^{2+} ion, which has a closed electronic shell, showed a moderate tendency toward distortion (Fig. 3). Although these relationships are shown in Figure 3 for the yttrium analogs, they have been observed similarly in the series of La, Nd, Sm, Gd, Dy, and Yb (unpublished data, J. Ito). The peculiar curvature of Cu analogs in the contour diagram of β angles, which was previously attributed to a possible error of ionic radius value (Ito, 1965), can now be interpreted as octahedral distortion.

Indexing of the X-ray powder diffraction data (Table 3) was facilitated by the intensities observed on 0-th, 1-st, 2-nd level single-crystal photographs recorded about the three crystallographic axes.

Mössbauer Spectroscopy

Mössbauer resonant absorption spectra of ^{57}Fe in yttrium gadolinite and calciogadolinite have been investigated. For comparison, the spectra of two synthetic åckermanite type phases $Sr_2FeSi_2O_7$ and $Ba_2FeSi_2O_7$ have also been studied. The spectra were recorded as usual with a 1024 channel analyzer operated in time mode in conjunction with an electromechanical velocity generator which moved the

TABLE 3. X-Ray Powder Data for Synthetic Gadolinites (Cu$K\alpha$ Radiation)

	Gadolinite*			Calciogadolinite**			$H_2Y_2Be_2Si_2O_{10}$ ***		
hkl	I/I	d_{obs}	d_{calc}	I/I	d_{obs}	d_{calc}	I/I	d_{obs}	d_{calc}
110	--	--	--	--	--	--	20	6.021	6.022
200	--	--	--	--	--	--	5	4.924	4.931
001	80	4.735	4.747	30	4.696	4.696	15	4.724	4.721
210	5	4.133	4.134	--	--	--	10	4.137	4.137
111	--	--	--	--	--	--	20	3.724	3.722
$\bar{1}11$	--	--	--	--	--	--	20	3.709	3.708
020	5	3.735	3.742	--	--	--	--	--	--
120	30	3.500	3.501	10	3.538	3.538	20	3.545	3.548
201	10	3.440	3.437	10	3.417	3.420	20	3.420	3.421
$\bar{2}01$	5	3.407	3.414		--	3.421	20	3.401	3.399
211	50	3.118	3.124		--	3.117	80	3.120	3.119
$\bar{2}11$	50	3.108	3.106		3.119	3.117	80	3.106	3.103
310	30	3.028	3.025	30	3.047	3.047	15	3.013	3.017
021	70	2.932	2.936	60	2.945	2.946	20	2.960	2.961
121	100	2.818	2.819	100	2.826	2.826	--	--	2.839
$\bar{1}21$	100	2.816	2.812		--	2.826	100	2.835	2.833
311	60	2.558	2.557	80	2.556	2.556	50	2.552	2.549
$\bar{3}11$	55	2.539	2.542	80	2.557	2.557	50	2.538	2.536
400	5	2.477	2.480	--	--	--	--	--	--
320	5	2.477	2.478	--	--	--	--	--	--
130	20	2.418	2.419	10	2.446	2.445	10	2.461	2.455
002	30	2.369	2.369	10	2.346	2.348	15	2.361	2.360
410	10	2.357	2.354	15	2.372	2.371	20	2.344	2.345
230	30	2.228	2.229	20	2.250	2.251	25	2.254	2.254
031	30	2.205	2.207	15	2.220	2.221	10	2.232	2.233
$\bar{3}21$	20	2.201	2.200	30	2.207	2.206	30	2.203	2.204
321	--	2.190	2.200		--	2.207	30	2.194	2.196
401	--	--	--	--	--	2.204	--	--	--
131	20	2.156	2.156	15	2.169	2.169	--	--	--
202	5	2.131	2.132	--	--	--	--	--	--
411	10	2.103	2.103	10	2.117	2.116	--	--	--
231	10	2.018	2.014	--	--	--	--	--	--
330	--	--	--	--	--	--	5	2.007	2.007
$\bar{2}31$	10	2.018	2.014	--	--	--	10	2.038	2.037
231	5	2.014	2.014	10	2.029	2.030	10	2.033	2.032
122	20	1.964	1.964		--	1.956	30	1.968	1.967
$\bar{1}22$	25	1.960	1.960	30	1.956	1.956	30	1.962	1.963
040	30	1.873	1.871	5	1.891	1.892	10	1.900	1.901
$\bar{3}12$	20	1.872	1.871		--	1.860	--	--	1.864
312	20	1.861	1.859	50	1.860	1.860	20	1.855	1.854
140	--	--	--		--	1.859	--	--	--
$\bar{3}31$	--	--	--				20	1.850	1.850
330	10	1.759	1.759	10	1.774	1.774	5	1.770	1.767
240	25	1.755	1.751	30	1.768	1.769	10	--	1.774
520	30	1.752	1.753	30	1.767	1.766	5	1.751	1.751
041	10	1.741	1.740	5	1.753	1.754	30	1.763	1.763
$\bar{4}02$	--	--	--				5	1.698	1.700
132	15	1.692	1.691	20	1.693	1.693	--	--	--
412	15	1.679	1.675			1.668	10	1.668	1.669
$\bar{4}12$	10	1.665	1.664	10	1.667	1.669	10	1.660	1.658
431	--	--	--	--	--	--	30	1.654	1.653
$\bar{4}31$	20	1.655	1.651	20	1.661	1.660	--	--	--
600	15	1.647	1.653	20	1.663	1.664	--	--	--
241	20	1.642	1.641	20	1.657	1.655	--	--	--
232	20	1.628	1.626	20	1.624	1.625	--	--	--
003	--	--	--	15	1.566	1.565	--	--	--
530	--	--	--	10	1.565	1.566	--	--	--
620	--	--	--	5	1.524	1.524	--	--	--

*$Fe^2Y_2Be_2Si_2O_{10}$, Monoclinic $P2_1/c$, a = 9.920(4), b = 7.484(2), c = 4.7474(7), β = 89°36'(2'), synthesized at 740°C, P_{H_2O} = 2 kbar and 48 hours, then heated at 1050°C in N_2 with 10% H_2 for 3 hours.

**$Fe^3CaYBe_2Si_2O_{10}$, Monoclinic $P2_1/c$, a = 9.988(2), b = 7.566(2), c = 4.696(1), β = 90°1'(2') synthesized at 1180°C in air for 48 hours.

***$H_2Y_2Be_2Si_2O_{10}$, Monoclinic $P2_1/c$, a = 9.861(4), b = 7.605(2), c = 4.720(2), β = 89°39'(2') synthesized at 600°C, P_{H_2O} = 2 kbar for 72 hours.

source (^{57}Co diffused into palladium). The experiments were carried out at constant acceleration and the velocity wave form was symmetric. The absorber densities varied between 2 and 4 mg natural iron per cm^2.

The absorbers were held at room temperature and in some cases also at liquid nitrogen temperature. The heights and widths of the quadrupole split doublets are presented in Table 4; the isomer shifts and nuclear quadrupole splittings are listed in Table 5. The spectra of yttrium gadolinite and calciogadolinite are shown in Figures 4 and 5, respectively.

The peak heights and widths of the Fe^{2+} doublet in yttrium gadolinite at 295 K are not equal. The peak at lower velocity is less intense and broader. The areas of the two peaks are about the same. At 77 K the effect is reduced. Similar asymmetries in heights and widths were also observed in the two iron silicates of the åckermanite type. Heights and widths of the Fe^{3+} doublet in calciogadolinite are nearly equal (Fig. 5).

The spectrum of calciogadolinite exhibits a small peak at zero velocity which represented 4 percent of the total resonant absorption area. The position of this peak would correspond to that of metallic iron in a superparamagnetic state. In $Ba_2FeSi_2O_7$ a peak due to some ferric iron was observed. The amount of Fe^{3+} ions was estimated to be a few percent of the total amount of iron. No ferric iron could be detected in the $FeY_2Be_2Si_2O_{10}$ and $Sr_2FeSi_2O_7$ samples.

In Table 5, the isomer shifts and nuclear quadrupole splittings of ^{57}Fe in iron containing gadolinites can be compared with those for åckermanite-type silicates, fayalite, and chain silicates. If we accept the rule that small quadrupole splittings of Fe^{2+} doublets at octahedral sites correspond to strong distortions of the coordination octahedron, we may conclude that the octahedron in yttrium gadolinite is at least as distorted as the $M4$ octahedron in grunerite. This is consistent with the trends in the isomer shifts. In chain silicates the isomer shifts can be correlated with the shortest Fe-O interatomic distance of the octahedron; the shorter that distance, the smaller the shift. Since the average Fe-O distance is generally more or less invariant, small isomer shifts reflect strong octahedral distortions.

In contrast to the situation of Fe^{2+} at octahedral sites, the quadrupole splitting of Fe^{3+} is expected to be in direct relation to the deviation of the coordination polyhedron from cubic symmetry. The unusually large splitting in $FeCaYBe_2Si_2O_{10}$ is indicative of a strongly distorted polyhedron. The value of 2.49 mm/sec (Table 5) is significantly greater than the Fe^{3+} splitting at $M1$ in diopside (Hafner and Huckenholz, 1971). The isomer shift supports this con-

TABLE 4. Peak Heights and Widths of ^{57}Fe Spectra

Compound	Valence state of iron	Absorber temperature (°K)	Low velocity peak		High velocity peak	
			Intensity[a]	Width[b] (mm/sec)	Intensity[a]	Width[b] (mm/sec)
$FeY_2Be_2Si_2O_{10}$	+2	295	0.430	0.39	0.570	0.28
		77	0.439	0.40	0.561	0.29
$FeCaYBe_2Si_2O_{10}$	+3	295	0.504	0.33	0.496	0.36
$Sr_2FeSi_2O_7$	+2	295	0.483	0.30	0.518	0.25
		77	0.497	0.31	0.503	0.26
$Ba_2FeSi_2O_7$	+2	295	0.467	0.39	0.533	0.28
		77	0.485	0.36	0.515	0.27

a) referred to total resonant absorption intensity of doublet.
b) full width at half height.

clusion since its smaller magnitude indicates a more covalent bonding state of Fe^{3+} in calciogadolinite as compared to diopside.

The quadrupole splittings of Fe^{2+} at the tetrahedral sites in $Sr_2FeSi_2O_7$ and $Ba_2FeSi_2O_7$ are small and also reflect strong distortions. The isomer shifts are comparatively small as expected for tetrahedrally coordinated Fe^{2+} ions.

The thermal shifts calculated from the isomer shifts at 77 K and 295 K in Table 5 are very close to -5.5×10^{-4} mm/s.K. In general, this value is in good agreement with other thermal shifts in silicates and seems to be nearly invariant for Fe^{2+} in widely different crystal structures.

Summary

Gadolinites can be described in terms of three end-members: gadolinite ($Fe^{2+}Ln^{3+}{}_2Be_2Si_2O_{10}$)–calciogadolinite ($Fe^{3+}CaLn^{3+}Be_2Si_2O_{10}$)–unnamed $H_2Ln^{3+}{}_2Be_2Si_2O_{10}$). We propose the following general formula: $H_{2x}Fe^{2+}{}_{2-x-y}Fe^{3+}{}_yCa_yLn^{3+}{}_{4-y}Be_4Si_4O_{20}$, $0 \leq y \leq 2$, $0 \leq x \leq 2$ and $0 \leq x+y \leq 2$. Here, Ln represents lanthanides and Y. The above three end-members are characterized by (1) the different occupants of the octahedral sites, namely Fe^{2+}, Fe^{3+}; and (2) the void with two OH. We believe that some structural water found in the existing chemical analyses is essential for the substitutions. The

TABLE 5. Isomer Shifts and Nuclear Quadrupole Splittings of ^{57}Fe Spectra

Compound	Valence state of iron	Site	Isomer shift[a,b] (mm/s)		Quadrupole splitting[b] (mm/s)	
			77°K	295°K	77°K	295°K
$FeY_2Be_2Si_2O_{10}$	+2	distorted octahedral	1.17	1.05	1.72	1.69
$FeCaYBe_2Si_2O_{10}$	+3	distorted octahedral	n.d.	0.36	n.d.	2.49
$Sr_2FeSi_2O_7$	+2	distorted tetrahedral	1.08	0.96	2.76	2.59
$Ba_2FeSi_2O_7$	+2	distorted tetrahedral	1.08	0.96	2.17	2.09
Fe_2SiO_4 Fayalite	+2	M1	n.d.	(1.16)[c]	n.d.	(2.84)[c]
		M2				
$FeSiO_3$ Orthoferrosilite	+2	M1	1.29	1.17	3.11	2.48
		M2	1.26	1.13	2.04	1.91
$Fe_7Si_8O_{22}(OH)_2$ Grunerite	+2	M1, M2, M3	1.30	1.16	3.14	2.79
		M4	1.20	1.07	1.56	1.55

a) referred to a metallic iron absorber at 295°K.
b) estimated total error ± 0.01 mm/sec.
c) average value of the two sites.

valencies are compensated mainly by vacancies in the octahedral sites.

The forty-four available chemical analyses from the literature have been plotted in a triangular diagram formed by the above end-members. They are plotted in Figure 1 in terms of molecular ratio of FeO, $FeO_{1.5}$ and $H_2O(+)$. Almost all the gadolinites including calciogadolinite from Tadachi, Japan, fall into the gadolinite region of the diagram. Only the calciogadolinite end member has been formed artificially at a high temperature (1250°C) in air. The gadolinite solid-solution series extend only half way from gadolinite to calciogadolinite in nature. It may reach all the way to the calciogadolinite end-member under certain conditions. One Russian analysis falls into the calciogadolinite region in Figure 1, but contains only 0.82 wt percent of CaO, which is too small to identify it as calciogadolinite. Solid-solution on the join calciogadolinite $H_2Ln_2Be_2Si_2O_{10}$ is probably partial.

Two gadolinites from Storna Tuna and Mälo, Sweden, and the unnamed mineral from Tuva, USSR, are the new species. The Tuva mineral is very close to the synthetic end-member $H_2Y_2Be_2Si_2O_{10}$, obtained hydrothermally at 600°C and P_{H_2O} = 2 kbar in this study.

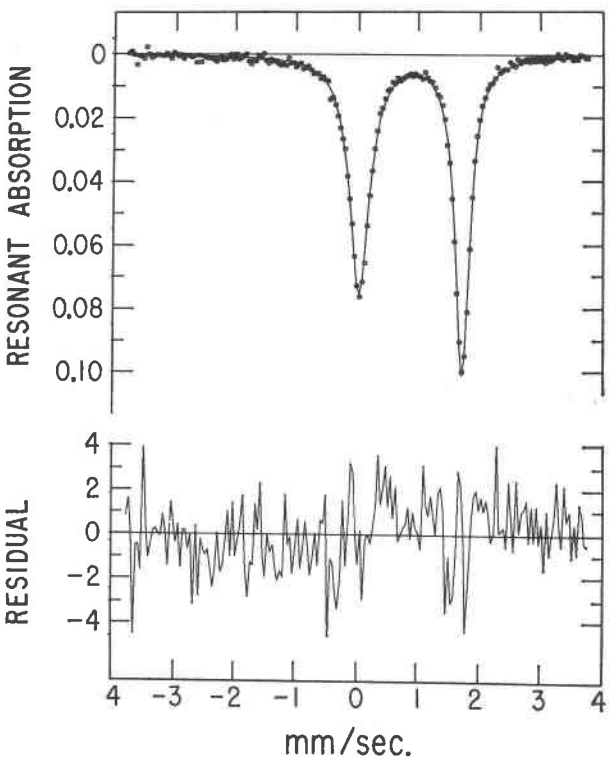

FIG. 4. Mössbauer absorption spectrum of ^{57}Fe in $FeY_2Be_2Si_2O_{10}$ at 295 K. Least-squares fit of two Lorentzians to quadrupole-split Fe^{2+} doublet.

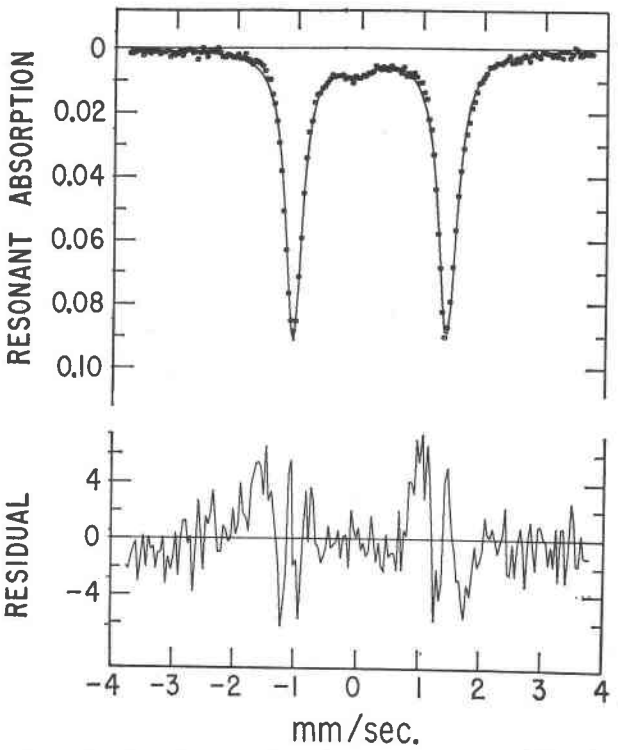

FIG. 5. Mössbauer absorption spectrum of ^{57}Fe in $FeCaYBe_2Si_2O_{10}$ at 295 K. Quadrupole-split Fe^{3+} doublet and weak absorption at 0 mm/sec (least-squares fit of three Lorentzians).

In synthetic gadolinites, various divalent ions can substitute completely in the octahedral ferrous iron sites, but only the Fe^{2+}-predominant gadolinites have been found in nature. Significant amounts of Mn^{2+} and Mg are often present, but not enough to establish an end-member. Absence of non-ferrous gadolinites in nature may be explained as the result of strong site preference by Fe^{2+} in the course of crystallization. Not only does the ionic radius of iron fit the octahedral site quite well, but in addition iron is preferentially partitioned into this site because of its inherent distortion. The relatively more rapid growth of the Cu^{2+} analogs as compared to other divalent ion analogs in a flux may also be due to the stability of Cu^{2+} in a strongly distorted site.

Acknowledgments

The writers thank Professor Clifford Frondel for his continuing interest and support, and H. Steffen Peiser of the National Bureau of Standards and Richard Beger for their editorial assistance.

Thanks are due to Professor G. V. Gibbs, Virginia Polytechnic Institute and State University, for his critical reading of the manuscript.

This work has been supported by the National Science Foundation Grant GH-335-76.

References

AHRENS, L. H. (1952) The use of ionization potentials, I. Ionic radii of the elements. *Geochim. Cosmochim. Acta,* **2,** 155–169.

ALEKSANDROVA, I. T., A. I. GINZBURG, I. I. KUPRIYANOVA, AND G. A. SIDORENKO (1966) *Geol. Mestorozhd. Redkikh Elementov.* Vses. Nauchn. Issled. Institute Mineral'n. Syr'ya, No. **26,** 66–90.

BAKAKIN, V. V., N. V. BELOV, S. V. BORISOV, AND L. P. SOLOVYEVA (1970) The crystal structure of nordite and its relationship to melilite and datolite-gadolinite. *Am. Mineral.* **55,** 1167–1181.

BRÖGGER, W. C. (1890) Die Mineralien der Syenitpegamatitgange der Südnorwegischen Augit und Nepheline Syenite. *Z. Kristallogr.* **16,** 134–158.

DES CLOIZEAUX, A., AND A. DAMOUR (1877) Note sur la forme crystalline propriétes optiques et la composition chimique de la homilite. *Ann. Chem. Phys.* **5,** 405–412.

DANA, E. S. (1900) *A System of Mineralogy,* 6th ed., John Wiley, N. Y., p. 511.

ENGSTRÖM, N. (1877) Undersökning af Några mineral, som Innehåla Sällsynta Jordarter. *Inaug. Diss., Upsala,* 1–39.

HAFNER, S. S., AND H. G. HUCKENHOLZ (1971) Mössbauer spectrum of synthetic ferri-diopside. *Nature Phys. Sci.* **233,** 9–11.

ITO, J. (1965) The synthesis of gadolinite. *Proc. Acad. Jap.* **41,** 404–407.

——— (1967) Synthesis of calciogadolinite. *Am. Mineral.* **52,** 1523–1527.

———, AND H. S. PEISER (1969) Distorted tetrahedra in strontium copper åckermanite. *J. Res. Natl. Bur. Stand.* **73A,** 69–74.

ITO, T., AND H. MORI (1953) The crystal structure of datolite. *Acta Crystallogr.* **6,** 24–32.

JAHN, H. A., AND E. TELLER (1937) Stability of polyatomic molecules in degenerate electronic states. I. Orbital degeneracy. *Proc. Royal Soc. London,* **A161,** 230–235.

LINDSTRÖM, G. (1874) Analys af gadolinit från Storna Tuna. *Geol. För. Förh.* **2,** 218–222.

NAGASHIMA, O., AND K. NAGASHIMA (1960) *Rare Elements Minerals from Japan,* p. 184–189. Japan Mineral Club Press, Kyoto, Japan.

NAKAI, T. (1938) On calciogadolinite, a new variety of gadolinite found in Tadachi, Nagano, Japan. *Bull. Chem. Soc. Jap.* **13,** 591–594. (*Mineral. Abstr.* **7,** 264 [1939])

PANT, A. K., AND D. W. J. CRUICKSHANK (1967) A reconsideration of the structure of datolite, $CaBSiO_4(OH)$. *Z. Kristallogr.* **125,** 286–297.

PAIKJULL, S. R. (1876) Homilite, ett mineral från Brevig, Norge, *G. För. Förh.* **3,** 229–232.

PAVLOV, P. V., AND N. V. BELOV (1959) The structure of herderite, datolite, and gadolinite determined by direct methods. *Kristallographiya,* **4,** 324–330.

PETERSSON, W. (1890) Studier ofver gadolinit. *Geol. För. Förh.* **12,** 275–347.

SEMENOV, E. I., V. D. DUSMATOV, AND N. S. SAMSONOVA (1963) Yttrium-beryllium minerals of the datolite group. *Kristallographiya,* **8,** 677–679.

SHANNON, R. D., AND C. T. PREWITT (1969) Effective ionic radii in oxides and fluorides. *Acta Crystallogr.* **B25,** 925–946.

Manuscript received, August 24, 1973; accepted for publication, February 6, 1974.